

Rebalance Of Mitophagy By Inhibiting LRRK2 Improves Parkinson's Disease-Related Colon Dysfunctions

Alessia Filippone, Deborah Mannino, Laura Cucinotta, Fabrizio Calapai, Lelio Crupi, Irene Paterniti and Emanuela Esposito*

Department of Chemical, Biological, Pharmaceutical and Environmental Sciences, University of Messina, Viale Ferdinando Stagno D'Alcontres, 31-98166 Messina, Italy

*Corresponding author:

Emanuela Esposito,

Department of Chemical, Biological, Pharmaceutical and Environmental Sciences, University of Messina, Viale Ferdinando Stagno D'Alcontres, 31-98166 Messina, Italy,

E-mail: eesposito@unime.it

Authors' contributions:

AF and EE planned the experiments; AF prepared the manuscript and analyzed the results; DM, LC, FC and LC performed experiments; IP and EE supervised the research.

Received Date: 09 Aug 2023

Accepted Date: 25 Aug 2023

Published Date: 31 Aug 2023

Citation:

Emanuela Esposito,
Rebalance Of Mitophagy By Inhibiting LRRK2 Improves
Parkinson's Disease-Related Colon Dysfunctions.
Journal of Pharmacology and Therapeutics 2023.

1. Abstract

Mutations in the leucine-rich repeat kinase 2 (LRRK2) gene are the most common genetic causes of Parkinson's disease (PD). Pathogenic mutations of LRRK2 cause increased autophosphorylation as well as Rab substrate GTPase phosphorylation which are associated with dopaminergic neuron death, impaired neurotransmission, and inflammatory response. Early preclinical studies suggested a protective role of LRRK2 inhibitors in PD patients and in in vivo models. Moreover, approximately 80% of PD patients suffer from gastrointestinal dysfunction so the treatment of gut symptoms has been recognized as an important part of the management of PD. Recent studies have demonstrated that mutations of LRRK2 contribute to an increase of intestinal disorders, further revealing that variants in LRRK2 genetically link these dysfunctions to PD. Based on these evidences, the aim of this study was to evaluate whether the selective inhibitor of LRRK2, PF-06447475 (PF-475), attenuates the PD

induced by 1-methyl-4-phenyl-1,2,3,6-tetrahydropyridine (MPTP) in Central Nervous System (CNS) and in the gastrointestinal system.

Animals received four intraperitoneal injections of MPTP (20 mg/kg) at two hours intervals in one day. After twenty-four hours PF-475 was administered intraperitoneally at different doses (2.5, 5 and 10 mg/kg) for seven days. Our results confirmed that LRRK2 targeting reduced brain α -Synuclein accumulation and modulated mitochondrial autophagic processes. Furthermore, PF-475 administration reduced pro-inflammatory markers like iNOS and COX-2 and α -Synuclein aggregates in colonic tissues PD-mice through the modulation of proteins involved in the mitoautophagy pathway such as p62, optineurin and LAMP2. In addition, LRRK2 inhibition suppressed MPTP-induced enteric dopaminergic neuronal injury through modulation of product 9·5 (PGP9.5) and neuron-specific enolase (NSE) and protected intestinal tight junction proteins, such as zonula occludens-1 and occludin disrupted by MPTP in the colon tissue. Together, these results indicate that selective inhibition of LRRK2 restores disruption of colonic integrity and enteric dopaminergic neurons in an MPTP-injected mouse PD model via the mitoautophagy pathway, suggesting that PF-475 may attenuate gastrointestinal dysfunction associated to PD.

2. Introduction

One of the most common chronic neurodegenerative diseases, known as Parkinson's disease (PD), affects 1% of adults older than 60 years and appear as distinctive motor symptoms such as resting tremor, bradykinesia, muscle rigidity, and postural balance disorders and nonmotor symptoms, like cognitive decline, depression, and anxiety. Symptomatology is rightly correlated to an abnormal accumulation of Lewy bodies (LBs), defined as neuroaxonal spheroids with a dense core largely containing α -synuclein and a loss of neurons in substantia nigra pars compacta (SNpc) [1]. Moreover, it has been proposed that gastrointestinal tract might be the site of initiation of PD or vice versa, suggesting that not only the Central nervous System (CNS) is impaired from motor and nonmotor symptoms, also the gastrointestinal system may take an active part in the pathophysiological changes PD-related and that results in a compromission of bowel and colon functionality surrounded by misfolded α -synuclein [2]. In order to treat PD, dopamine drug therapy and brain surgical electrical stimulation are currently the most common clinical treatments for symptomatic conditions. However, these methods can only improve PD symptoms and cannot stop the disease from getting worse also outside the brain for instance throughout the gastrointestinal system.

Thus, it is necessary to investigate alternative effective approaches that can not only improve motor and nonmotor symptoms but also attenuate

the accumulation of misfolded α -synuclein in CNS and gastrointestinal system both [3]. Indeed, α -synuclein deposition occurs in the myenteric and submucosal plexuses and mucosal nerve fibres of PD subjects, with a clear deposition throughout the entire enteric nervous system. In several number of PD cases, it has been found specific mutation in genes of various functions including PINK1, Parkin, α -synuclein and also leucine repeat kinase 2 (LRRK2). LRRK2 is a 286 kDa multidomain protein belonging to the Roco family of G-proteins. Its structure consists of N-terminal armadillo, ankyrin, and LRR repeats followed by a small GTPase like domain called Roc (Ras of complex proteins), a COR (C-terminal of Roc), a kinase, and a WD40 domain. Particularly, linked mutations to LRRK2 gains its kinase activity contributing to the α -synuclein propagation and aggregation in SNpc and in gastrointestinal system [4]. As such, LRRK2 inhibitors have been reported as tools to pharmacologically and structurally inhibit kinase activity and to cross the brain blood barrier (BBB) driving diverse signaling pathways and repairing cellular processes such as cytoskeleton remodeling, adequate vesicular trafficking, functional control of autophagy and mitochondria [5,6]. Mitochondrial dysfunctions have been reported in the pathogenesis of both sporadic PD and familial Parkinsonism with a reduction of its dynamics about 40% in the SNpc of 1-methyl-4-phenyl-1,2,3,6-tetrahydropyridine (MPTP)-induced mice and PD patients.

Indeed, the highly controlled fission/fusion process of misfolded proteins and organelles that occur in mitochondria results defective in PD because of the presence of an extensive damage to mitochondrial segments that cannot be repaired for local repair mechanism and thus undergo recycling through autophagy and lysosome system (ALS) [7]. The mitochondrial quality control failure implicates misfolded proteins and organelles to being degraded from ALS that became engulfed and non-stop recruit autophagy selective activators like microtubule associated protein 1 light chain 3 (MAP-LC3), optineurin and nuclear factor kappa B subunit (NF- κ B) to form autolysosomes and ultimately degrade cargos [8]. In this context, it is still unclear how LRRK2 or its inhibition could contribute to mitochondrial dysfunction in PD and in the gastrointestinal system. Here, we aimed to evaluate the mechanism of action of LRRK2 in modulating mitochondrial and ALS systems in an *in vivo* model of MPTP induced PD by preventing CNS neurodegeneration and pathological related consequences to the gastrointestinal system.

3. Materials And Methods

3.1. Materials

PF06447475 (abbreviated as PF-475) was purchased from MedChemExpress LLC (1 Deer Park Dr, Suite Q, Monmouth Junction, NJ 08852, USA; # HY-12477). All stock solutions were prepared in nonpyrogenic saline (0.9% NaCl; Baxter, Liverpool, UK). Unless otherwise stated, all compounds were obtained from Sigma-Aldrich (Milan, Italy).

3.2. Animals

CD1 male mice (25–30 g; 6–8 weeks of age) were purchased from Envigo

(Milan, Italy). The mice were placed in a controlled environment and were fed with standard rodent food and water *ad libitum*. The animals were housed in stainless steel cages in a room maintained at 22 ± 1 °C with a cycle of 12 h of light and 12 h of dark. The animal study was performed in accordance with Italian regulations on the use of animals (D.M.116192) and Directive legislation (EU) (2010/63/EU) amended by Regulation (EU) 2019/1010. The animal protocol was approved by Italian Committee (n° 399/2019-PR released on 2019).

3.3. Induction of PD Mouse Model

Adult male CD1 mice received four intraperitoneal injections of 1-methyl-4-phenyl-1,2,3,6-tetrahydropyridine (MPTP) (20 mg/kg; Sigma-Aldrich, St. Louis, MO) in saline at 2 h intervals in 1 day and the total dose for each mouse was 80 mg/kg. Starting 24 h after the first MPTP injection, animals received intraperitoneal administration of PF-475 at doses of 2.5 mg/kg, 5 mg/kg and 10 mg/kg respectively. PF-475 was administered once daily until 7 days after the MPTP injection. PF-475 was dissolved in dimethyl sulfoxide (DMSO) and diluted with 0.9% saline to a final concentration of <1% DMSO. 7 days after MPTP injection brains, bowel and colon were harvested, sectioned, and used for further analysis.

3.4. Experimental Groups

Animals were randomly divided as follows:

Group 1: Sham + vehicle; vehicle solution (saline) was injected intraperitoneally for 7 consecutive days (N = 10);

Group 2: Sham + PF-475 2.5 mg/kg; like Sham + vehicle group, in addition mice was administered intraperitoneally with PF-475 2.5 mg/kg for 7 consecutive days starting 24 h after vehicle solution injection (N = 10);

Group 3: Sham+PF-475 5 mg/kg; like Sham + vehicle group, in addition mice was administered intraperitoneally with PF-475 5 mg/kg for 7 consecutive days starting 24 h after vehicle solution injection (N = 10);

Group 4: Sham+PF-475 10 mg/kg; like Sham + vehicle group, in addition mice was administered intraperitoneally with PF-475 10 mg/kg for 7 consecutive days starting 24 h after vehicle solution injection (N = 10);

Group 5: MPTP+vehicle: mice received intraperitoneally MPTP solution during the first day, and saline intraperitoneal administration for 7 consecutive days starting 24 h after MPTP injection.

Group 6: MPTP+PF-475 2.5 mg/kg; like MPTP + vehicle group, in addition mice was administered intraperitoneally with PF-475 2.5 mg/kg for 7 consecutive days starting 24 h after first MPTP injection (N = 10);

Group 7: MPTP+PF-475 5 mg/kg; like MPTP + vehicle group, in addition mice was administered intraperitoneally with PF-475 5 mg/kg for 7 consecutive days starting 24 h after first MPTP injection (N = 10);

Group 8: MPTP+PF-475 10 mg/kg; like MPTP + vehicle group, in addition mice was administered intraperitoneally with PF-475 10 mg/kg for 7 consecutive days starting 24 h after first MPTP injection (N = 10).

The PF-475 route and doses of administration was based on previous *in vivo* study [9]. The minimum number of mice for every technique was estimated with the statistical test “ANOVA: Fixed effect, omnibus

one-way” with G-power software. Data regarding sham mice subjected to intraperitoneally treatment with PF-475 at different doses (2.5, 5 and 10 mg/kg) are not shown because of no significant changes reported in Sham + PF-475 2.5, 5 and 10 mg/kg treated mice compared to the Sham + vehicle mice.

3.5. Western Blot Analysis

For western blot analysis, the brain, colon and bowel tissues were surgically isolate. Tissue samples were processed as previously reported by Filippone et al [9]. The expression of leucine-rich repeat kinase 2 (LRRK2), phosphorylated LRRK2 at Serine935 (p-Ser935), cyclooxygenase-2 (COX-2), inducible nitric oxide synthase (iNOS), α -Synuclein, protein gene product 9.5 (PGP9.5), neuron specific enolase (NSE), ubiquitin-binding protein p62 (p62), optineurin (OPT), lysosome-associated membrane protein-2 (LAMP2), and tumor necrosis factor- α (TNF- α) were quantified in cytosolic proteins fractions. The following primary antibodies were used: anti-LRRK2 (1:1000 Abcam, ab-133474), anti-phosphorylated LRRK2 at Serine935 (1:1000 Abcam, ab-133450) anti-iNOS (1:500; Santa Cruz Biotechnology, Dallas, TX, USA; sc-7271); anti-COX2, anti- α -Synuclein (1:500; Santa Cruz Biotechnology, Dallas, TX, USA; sc-) anti- PGP9.5 (Elabscience, Cat no. E-AB-53097); anti-NSE (Invitrogen PA5-94940); anti-p-62 (1:1000, Abcam, ab91526), anti-optineurin (1:500; Santa Cruz Biotechnology, Dallas, TX, USA; sc-166576); anti-LAMP2 (Invitrogen, MA1-205); anti-TNF- α (1:500; Santa Cruz Biotechnology sc-52746). To confirm that the samples contained an equal protein concentration, membranes were incubated with primary anti- β -actin antibody (1:500; sc-47778; Santa Cruz Biotechnology, Dallas, TX, USA). Finally, signals were revealed by enhanced chemiluminescence (ECL) detection system reagent according to the manufacturer’s instructions (SuperSignal West Pico Chemiluminescent Substrate, Thermo Fisher Scientific, Waltham, MA, USA). The relative expression of the protein bands was quantified by densitometry with BIORAD ChemiDoc™XRS+ software and standardized to β -actine levels as internal control.

3.6. Measurement Of Dopamine, 3,4-Dihydroxyphenylacetic Acid (DOPAC), And Homovanilic Acid (HVA) Levels In The Striatum

Dopamine and its metabolites, 3,4-dihydroxyphenylacetic acid (DOPAC) and homovanilic acid (HVA) were quantified as previously showed [10]. Measurements were performed via high performance liquid chromatography (HPLC) with electrochemical detection, using 0.15 M monochloroacetic acid, pH 3.0, and 200 mg/L sodium octyl sulfate, 0.1 mM EDTA, 4% acetonitrile, and 2.5% tetrahydrofuran as mobile phase. Data were collected and processed on a Dynamax (Rainin Instruments) computerized data manager.

3.7. Enzyme-Linked Immunosorbent Assay (ELISA Kit)

The ELISA kit assay was performed on the protein extract of bowel and colon samples to determine the concentration of proinflammatory cytokine according to manufacturer’ instructions (Mouse IL-1 β ELISA Kit, Abcam, ab197742).

3.8. Histological Evaluation

Histological analyses were performed as previously described [11]. Briefly, after the sacrifice, colon and bowel tissues were fixed in 10% (w/v) PBS-buffered formaldehyde solution at 25 °C for 24 h. After a dehydration process through a scale of increasing concentrations of alcohols and xylene, tissues were included in paraffin (Bio-Optica, Milan, Italy) and subsequently cut under the microtome obtaining 7 μ m thick sections. For morphological analyses, slides were stained with Hematoxylin/Eosin (H&E, Bio-Optica, Milan, Italy) to assess histological alterations, edema, and neutrophilic infiltration. We used the following morphologic criteria for the histological analysis: score 0 no morphologic damage; score 1 focal epithelial edema as well as necrosis; score 2 diffuse inflammation and necrosis of villous area; score 3 presences of neutrophilic infiltration in submucosa area; score 4 necrosis and neutrophil infiltration; score 5 vast neutrophilic infiltrations and bleeding. All sections were examined using a Nikon Eclipse Ci-L microscope. The results of the histological examinations were displayed at 20x magnification (50 μ m scale bar) and 40x magnification (20 μ m scale bar).

3.9. Immunohistochemistry Analysis

The immunohistochemistry analysis was performed as described before [12]. The colon sections of 7 μ m were used for immunohistochemical staining. Sections were incubated overnight (O/N) with the following primary antibodies: anti-PGP9.5 (Elabscience, Cat no. E-AB-53097) and α -synuclein (1:100; sc-7011; Santa Cruz Biotechnology, Dallas, TX, USA). Then, the sections were washed with PBS and incubated with secondary antibody for 1 h. The reaction was revealed by a chromogenic substrate (brown DAB), and counterstaining with nuclear fast red. All stained sections were observed and analyzed in a blinded manner with a Nikon Eclipse Ci-L microscope. Immunohistochemistry results were showed at 20x magnification (50 μ m scale bar) and 40x magnification (20 μ m scale bar).

3.10. Immunofluorescence Analysis

Colon sections were processed for immunofluorescence staining as previously described [12]. Sections were incubated with anti-ZO-1 (1:100; Santa Cruz Biotechnology, Dallas, TX, USA; sc-33725) or anti-occludin (1:100; Santa Cruz Biotechnology, Dallas, TX, USA; sc-133256) antibodies in an O/N humidified chamber. The sections were then incubated with a secondary antibody, a fluorescein-isothiocyanate (FITC) conjugated anti-mouse Alexa Fluor-488 antibody (1:1000 v/v Molecular Probes, Altrincham, UK), for 3 hours at room temperature. Finally, after washing with PBS, nuclei were stained by adding 2 μ g/mL 40,60-diamidino-2-phenylindole (DAPI; Hoechst, Frankfurt, Germany). Sections were observed at 40 \times magnification using a Nikon Eclipse Ci-L microscope. For each antibody analyzed, positive cells were counted stereologically on the sections by examining the most brightly labeled pixels and applying settings that allowed clear visualization of structural details. The same settings were used for all images obtained from the other samples which were processed in parallel.

3.11. Lactulose/Mannitol (Lac/Man) Test To Evaluate Gut Permeability

The lactulose and mannitol test (Lac/Man) was performed as previously described [13]. Lac/Man test was made using standard doses of sugars to detect intestinal permeability. Lactulose, at concentrations of 5 mg and mannitol, at concentrations of 12.5 mg, were administered simultaneously to each mouse by using an oral gavage. To collect urine, mice were isolated individually in metabolic cages. Urine from mice was collected whole over 24 hours for sugar analyzes and stored at -80°C for HPLC analysis. The urinary levels of both sugars were calculated as a percentage of the ingested dose in mg.

3.12. Determination Of Fecal Weight

Determination of fecal weight was performed as constipation-related indicator [14]. Fecal weight was measured every day from day one to day seven.

3.13. Transepithelial Electrical Resistance (TEER) Measurement

Barrier integrity was assessed with transepithelial electrical resistance (TEER), a quantitative measure of the electrical ohmic resistance of intestinal tissue. STX2 electrodes and a 4-point measurement system on Transwell permeable inserts were used for the TEER method [doi.org/10.3390/ijms24043122]. To measure TEER, two sets of electrodes were used; one was placed in the basolateral compartment and the other was placed in the apical compartment. Human normal colonocytes (NCM460 cell line) [15] were seeded at a high density (1.25×10^5 cells/cm²) on clear polyester Transwell permeable supports (Corning Glass) in growth medium. Growth medium (apical and basal) was changed every day before and during treatments. PF-475 (0.5, 1, 3 μM) was added to the culture medium. An EVOM epithelial volt/ohmmeter with STX electrodes (rods) (World Precision Instruments, Sarasota, FL, USA) was used to measure TEER.

4. Results

4.1. LRRK2 inhibition reduced α -syn aggregates and prevented dopamine depletion after MPTP intoxication in mouse brain tissue

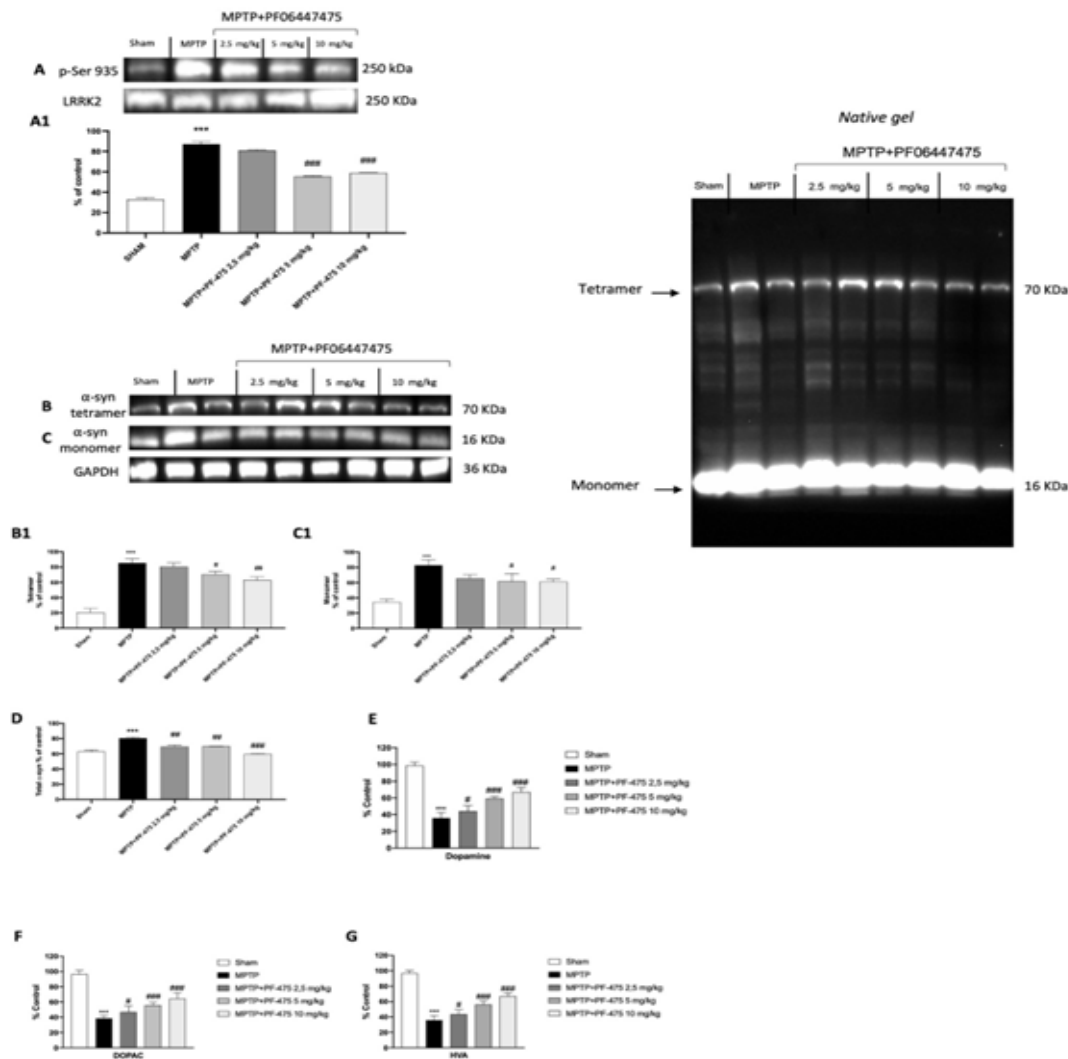
We performed immunoblot analysis on the brain protein extract of mice from each experimental group to demonstrate the selective inhibition of LRRK2 following PF-475 treatment. As expected, LRRK2 expression was significantly higher in brain tissues of MPTP-injected mice compared to sham mice, while intraperitoneal treatment with PF-475 at the highest doses of 5 mg/kg and 10 mg/kg significantly reduced LRRK2 expression compared with MPTP-injected mice (figure 1 A, see densitometric analysis panel A1). In contrast, intraperitoneal treatment with PF-475 at the lowest dose of 2.5 mg/kg was unable to downregulate LRRK2 expression in the brain of MPTP-injected mice (figure 1 A, see densitometric analysis panel A1). Moreover, since the accumulation of α -syn in dopaminergic neurons is a critical marker of PD, we wanted to evaluate the expression

of this protein to confirm the key role of LRRK2 in the neurodegenerative process and that its inhibition represents a potential therapeutic target for the treatment of the PD.

Quantitative Western blot analysis of brain samples revealed decreased α -Syn tetramers and monomers following PF-475 treatment at the highest doses of 5 mg/kg and 10 mg/kg compared to MPTP-injected mice (figure 1 panel B and panel C, see densitometric analysis panel B1 and C1, respectively). Consistently, total densitometric analysis of α -Syn monomers and tetramers (figure 1 panel D) showed a significant increase of α -Syn aggregates in brain samples of MPTP-injected mice compared to sham mice, while a dose-dependent reduction of total α -Syn aggregates was observed in mice treated with PF-475 at doses of 2.5 mg/kg, 5 mg/kg and 10 mg/kg compared to MPTP-injected mice. Degeneration of the nigrostriatal innervation leads to dopaminergic cell loss which is a typical feature of the pathogenesis of PD. Our results confirmed the neuroprotective role of the LRRK2 antagonist, PF-475, by evaluating striatal levels of dopamine and its metabolites such as 3,4-dihydroxyphenylacetic acid (DOPAC) and homovanilic acid (HVA). MPTP intoxication significantly reduced striatal dopamine (figure 1 panel E), DOPAC (figure 1 panel F) and HVA (figure 1 panel G) levels compared to sham mice. Treatment with PF-475 at doses of 2.5 mg/kg, 5 mg/kg and 10 mg/kg showed a significant recovery of the levels of dopamine and its metabolites in a dose-dependent manner. Collectively, these results supported the neuroprotective capabilities of the LRRK2 selective inhibitor, PF-475 in a mouse model of MPTP-induced nigrostriatal degeneration.

Figure 1: Effect of LRRK2 inhibition on α -syn aggregates and dopamine in mouse brain.

Representative Western blot of phosphorylated LRRK2 at Serine 935 protein expression level in cytosolic fraction of brain tissues after MPTP intoxication and PF-475 treatments (A, see densitometric analysis A1). Representative Western blot of α -syn tetramer and monomer protein expression level in brain tissues after MPTP intoxication and PF-475 treatments (B,C; see densitometric analysis B1, C1, respectively). Total densitometric analysis of α -Syn monomers and tetramers (D). MPTP-injected animals exhibited a considerable loss of dopamine and its metabolites, compared to the Sham mice; contrarily, treatment with PF-475 in a dose-dependent manner 2.5 mg/kg, 5 mg/kg and 10 mg/kg increased metabolites levels (E-G). Data are representative of at least three independent experiments. Values are means \pm SEM. One-way ANOVA test. *** $p < 0.001$ vs Sham; # $p < 0.05$ vs MPTP; ## $p < 0.01$ vs MPTP; ### $p < 0.001$ vs MPTP.



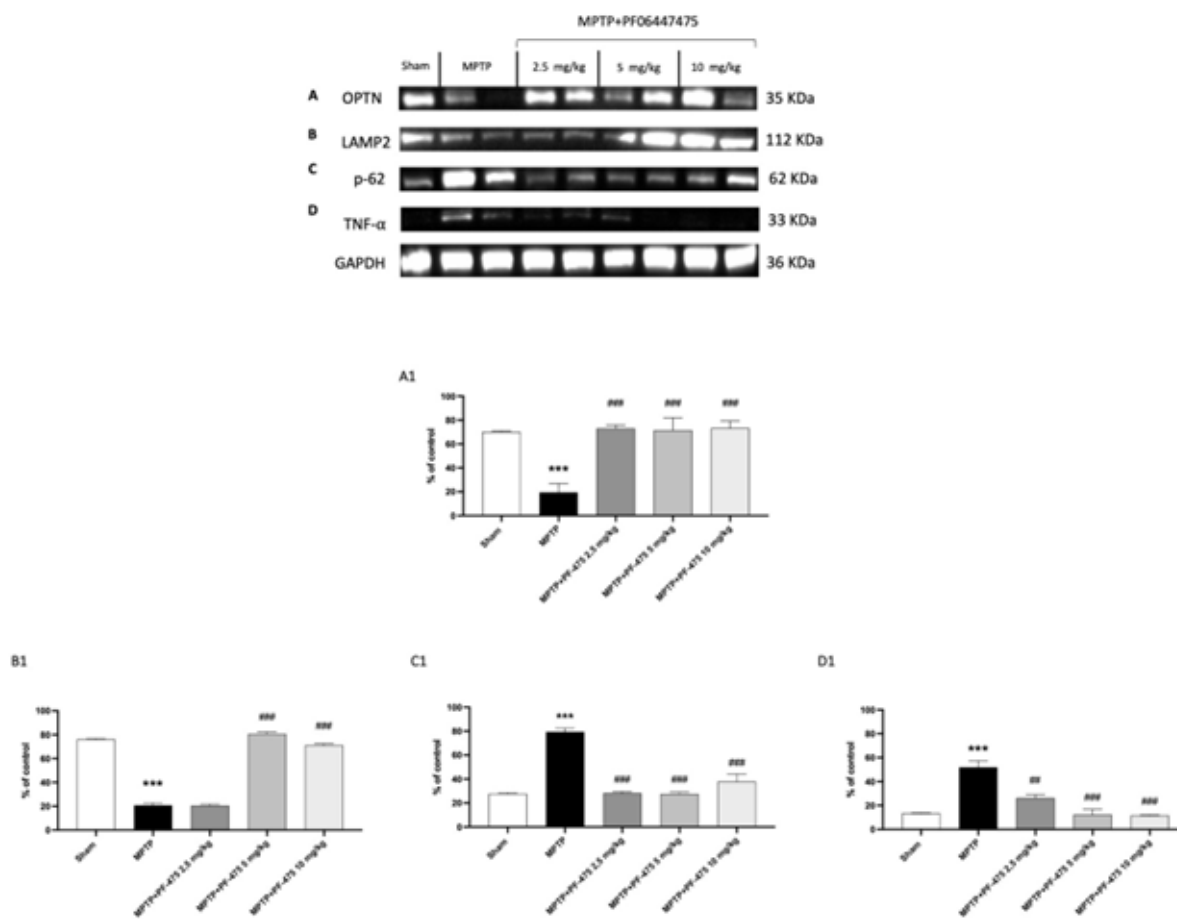
4.2. LRRK2 Inhibition Modulated Mitophagy Pathway In Brain Tissue

Overexpression of LRRK2 involved in PD pathogenesis leads to increased kinase activity. Increased kinase activity of LRRK2 reduces the interaction between the optineurin autophagy receptor (OPTN) with ubiquitous mitochondrial outer membrane (OMM) proteins resulting in a negative impact on mitophagy [16]. Indeed, OPTN plays a key role in mitophagy not only targeting dysfunctional mitochondria to autophagosomal membranes, but also facilitating the formation of autophagosomal membrane [17]. Our results demonstrated that MPTP-injected mice showed a compromised mitophagy demonstrating low levels of OPT compared to sham mice. PF-475 treatment significantly restored the mitophagy pathway through the significant increase of OPT expression compared to MPTP-injected mice (figure 2 A, see densitometric analysis panel A1). The process of mitophagy is modulated by other different proteins including LAMP2 and p62. LAMP2, a lysosomal membrane protein, plays an important role in lysosomal stability as well as in autophagy. The overexpression of LAMP2 increases autophagy activity, and this effect is accompanied by decreased levels of p62 [18]. As shown in Figure 2 we found that LAMP2 expression in MPTP-injected mice was significantly reduced compared to sham mice (figure 2 B, densitometric analysis panel B1), conversely, p62

expression was significantly increased in MPTP-injected mice compared with sham mice (figure 2 C, densitometric analysis panel C1). However, treatments with PF-475 at the doses of 5 mg/kg and 10 mg/kg significantly increased LAMP2 expression compared to MPTP mouse. On the other side, a significant reduction of p62 following PF-475 treatment at the doses of 2.5 mg/kg, 5 mg/kg and 10 mg/kg was observed compared with the MPTP group (Figure 2 panel C, see densitometric analysis panel C1). These data could indicate a restoration of increased autophagic flux in brain tissue following PF-475 treatment. In addition, impaired autophagic flux increases pro-inflammatory mediators such as tumor necrosis factor- α (TNF- α), which is highly toxic to dopaminergic neurons and a major mediator of neuroinflammation in PD [19]. Our results demonstrated an increased expression of the pro-inflammatory cytokine TNF- α in MPTP-injected mice compared with sham mice. In contrast, treatment with PF-475 significantly reduced TNF- α expression levels at doses of 5 mg/kg and 10 mg/kg compared to MPTP-injected mice (figure 2 D, see score panel D1).

Figure 2: Effect of LRRK2 inhibition on mitophagy pathway in brain. Cytosolic protein fractions of brain tissues were used to evaluate mitophagic protein expression such as OPT, LAMP2 and p62 and pro-

inflammatory cytokine TNF- α after MPTP intoxication and PF-475 treatments. Representative Western blot of mitophagic protein are shown (A,B,C), see densitometric analysis (A1, B1 and C1, respectively). Western blot of pro-inflammatory cytokine TNF- α are shown (D, see densitometric analysis D1). Data are representative of at least three independent experiments. Values are means \pm SEM. One-way ANOVA test. *** p < 0.001 vs Sham; ## p < 0.01 vs MPTP; ### p < 0.001 vs MPTP.

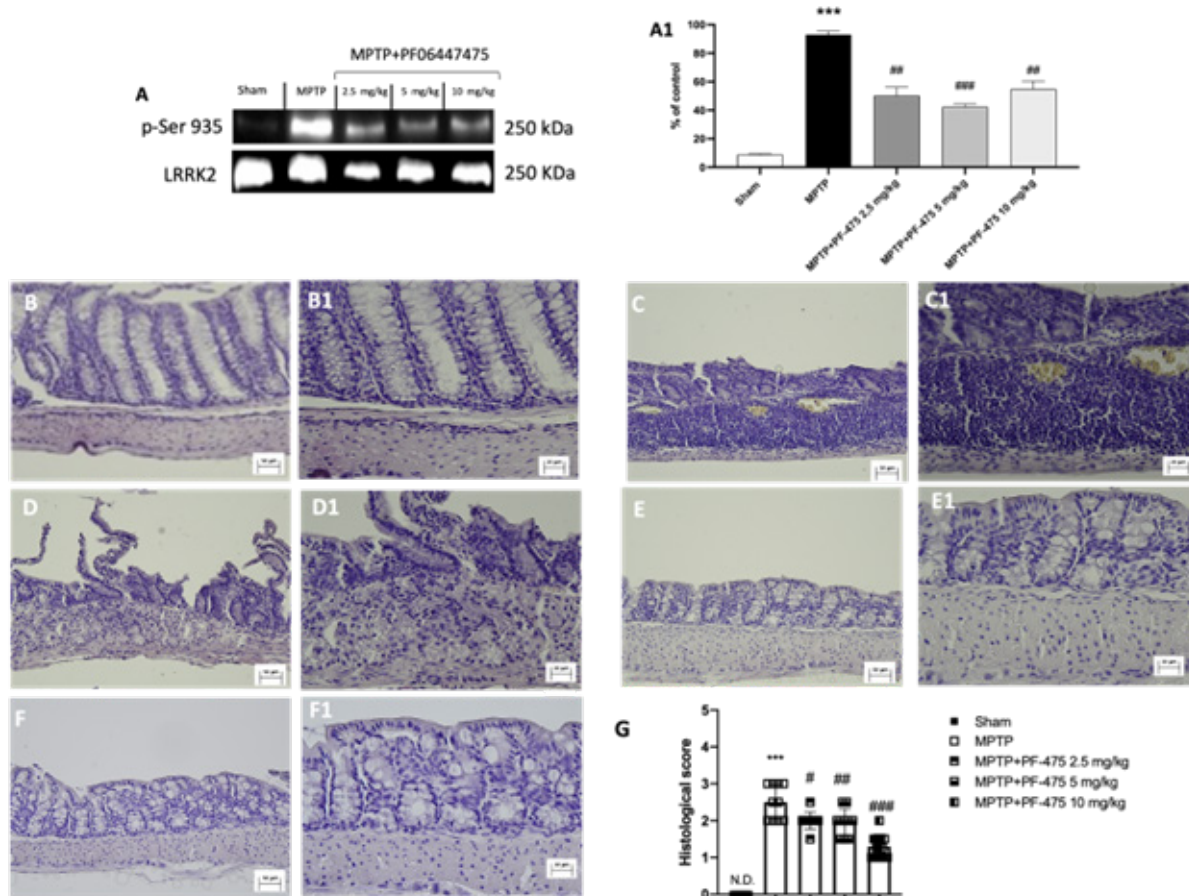


4.3. LRRK2 Inhibition Attenuated Histological Damage In MPTP-Injected Mouse Bowel

Previous studies showed that LRRK2 mutations genetically link Parkinson's disease to inflammatory bowel disease [20,21]. In this study we aimed to examine the effects of the LRRK2 selective antagonist, PF-475 on intestinal tissue of PD mouse. Expression of LRRK2 phosphorylation at Ser-935 in intestinal tissues was measured by Western blot analysis and was found to be elevated in bowel tissues of MPTP-injected mice compared to sham mice. PF-475 at doses of 2.5 mg/kg, 5 mg/kg and 10 mg/kg significantly reduced LRRK2 phosphorylation at Ser-935 expression compared to MPTP-injected mice (figure 3 panel A, densitometric analysis panel A1). Furthermore, the histological effects of PF-475 in MPTP-injected mice were measured using H&E staining. Mice in the MPTP group showed disruption of epithelial architecture and increased number of inflammatory cells (figure 3 panel C, 20x magnification C1) compared to sham mice (figure 3 panel B, 20x magnification B1). PF-475

prevented these signs of intestinal inflammation at doses of 2.5 mg/kg (figure 3 panel D, 20x magnification D1), 5 mg/kg (figure 3 panel E, 20x magnification E1) and 10 mg/kg (figure 3 panel F, 20x magnification F1) compared to MPTP-injected mice.

Figure 3: Effects of PF-475 treatments on histological damage in MPTP-injected mouse bowel. Representative Western blot of phosphorylated LRRK2 at Serine 935 protein expression level in cytosolic fraction of bowel tissues after MPTP and PF-475 treatments (A, see densitometric analysis A1). Hematoxylin and eosin staining of Sham group (B, B1), MPTP group (C, C1), PF-475 2.5 mg/kg treatments after MPTP (D,D1), PF-475 5 mg/kg treatments after MPTP (E,E1) and PF-475 10 mg/kg treatments after MPTP (F,F1), see histological score (G). Data are representative of at least three independent experiments. Values are means \pm SEM. One-way ANOVA test. *** p < 0.001 vs Sham; # p < 0.05 vs MPTP; ## p < 0.01 vs MPTP; ### p < 0.001 vs MPTP.

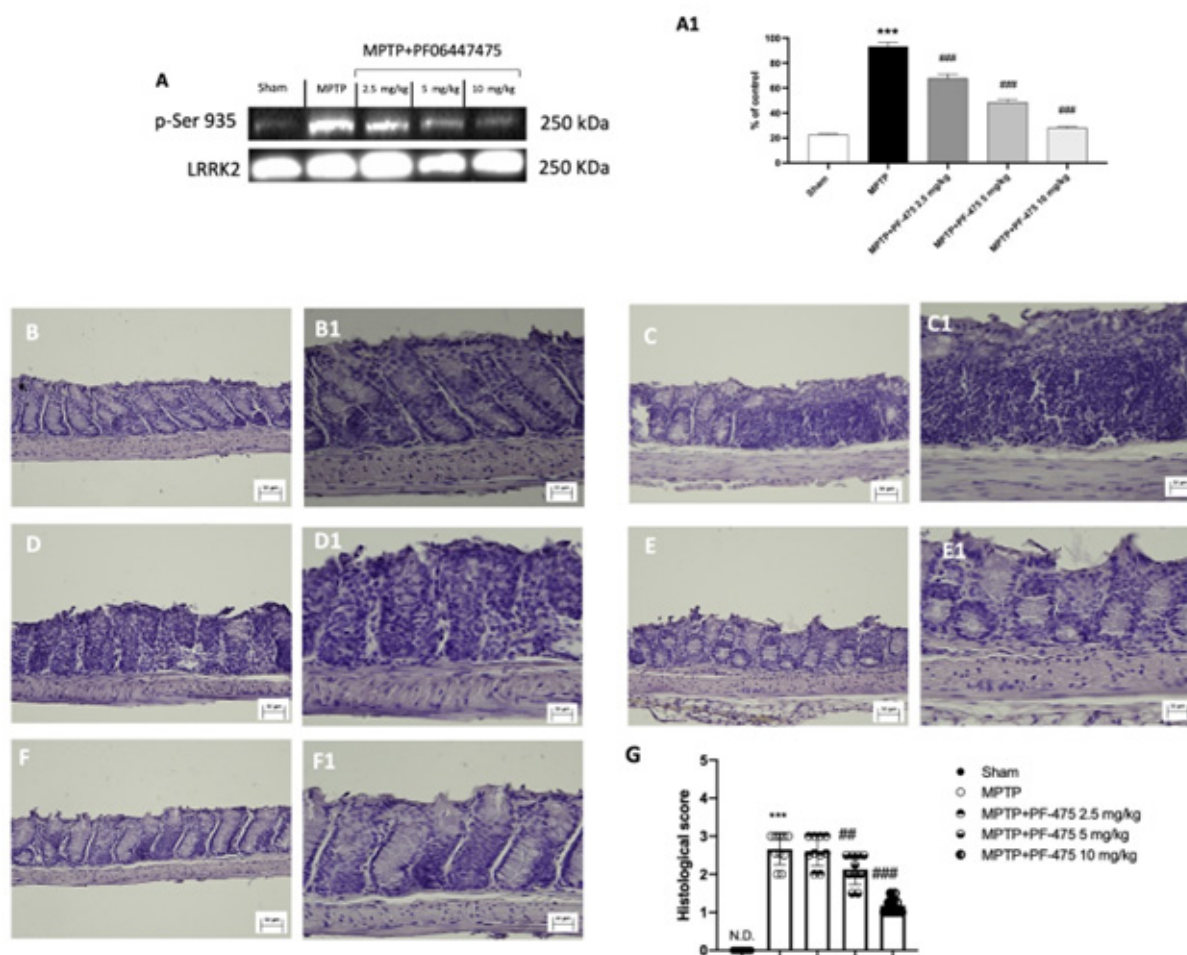


4.4. LRRK2 Inhibition Ameliorated Colon Damage In MPTP-Injected Mouse

Study of LRRK2 phosphorylation at Ser-935 expression in colonic tissues of MPTP-treated mouse demonstrated overexpression of this protein kinase after MPTP intoxication compared to sham animals (figure 4 panel A, see densitometric analysis panel A1). Intraperitoneal treatment with PF-475 in a dose-dependent manner significantly reduced phosphorylation of the kinase (figure 4 panel A, see densitometric analysis panel A1). Furthermore, the MPTP group showed more severe colonic inflammation, loss of crypt architecture, edema, and the extent of infiltration with inflammatory cells damage extending in the submucosa (figure 4 panel C, 20x magnification C1) layers than the sham group (figure 4 panel B, 20x magnification B1). Instead, treatment with PF-475 at the highest doses of 5 mg/kg (figure 4 panel E, 20x magnification E1) and 10 mg/kg (figure 4 panel F, 20x magnification F1) significantly improved tissue architecture and reduced inflammation compared to MPTP-injected mouse. Instead, no significant difference was found following treatment with PF-475 at

the lower dose of 2.5 mg/kg in reducing the histological score (figure 4 panel D, 20x magnification D1). Taken together, these results suggested for the first time, an involvement of LRRK2 in MPTP-induced intestinal damage and demonstrated how selective inhibition of LRRK2 through PF-475 administration could restore colonic damage in MPTP mice.

Figure 4: Effects of PF-475 treatments on histological damage in MPTP-injected mouse colon. Representative Western blot of phosphorylated LRRK2 at Serine 935 protein expression level in cytosolic fraction of colon tissues after MPTP and PF-475 treatments (A, densitometric analysis A1). Hematoxylin and eosin staining of Sham group (B, B1), MPTP group (C, C1), PF-475 2.5 mg/kg treatments after MPTP (D, D1), PF-475 5 mg/kg treatments after MPTP (E, E1) and PF-475 10 mg/kg treatments after MPTP (F, F1), see histological score (G). Data are representative of at least three independent experiments. Values are means \pm SEM. One-way ANOVA test. *** $p < 0.001$ vs Sham; ## $p < 0.01$ vs MPTP; ### $p < 0.001$ vs MPTP.



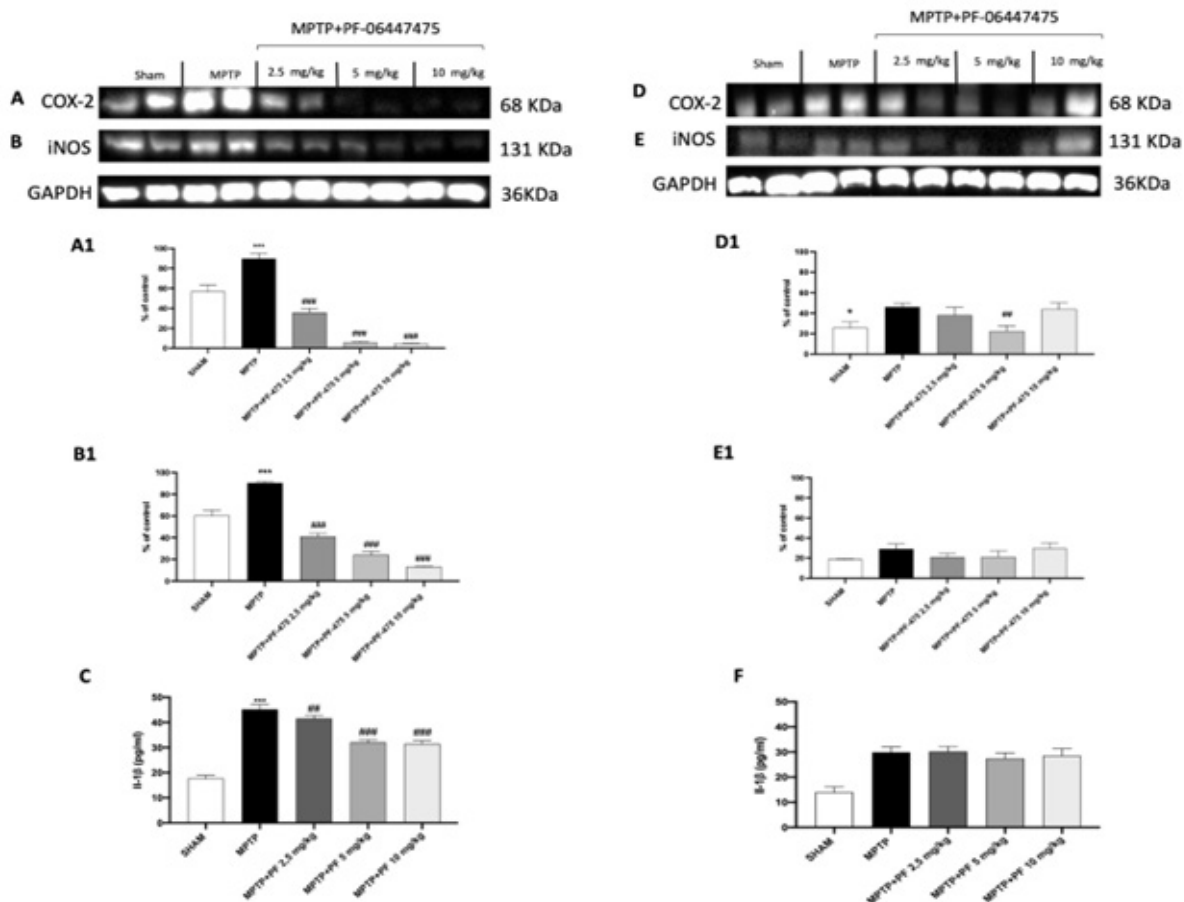
4.5. Effect Of PF-475 On Pro-Inflammatory Response Induced By MPTP Intoxication In Colon And Bowel Tissues

In parallel with CNS inflammation during PD, recent studies indicate similar processes at peripheral sites [22]. In particular, increases in proinflammatory markers levels in the colon and intestine provide strong evidence of gastrointestinal inflammation in patients with PD [23]. Moreover, previous studies reported that MPTP induced the inflammatory response in mouse colon and intestinal section [24,25]. We used Western blot analysis and ELISA assay to evaluate the effects of PF-475 on the inflammatory markers in the colon and bowel tissues following MPTP intoxication. The results showed that, in MPTP mouse, the expression of pro-inflammatory enzymes such as iNOS and COX-2 in colon tissues increased significantly compared to sham animals (figure 5 panel A and B, see densitometric analysis panel A1 and B1, respectively). Following intraperitoneal treatment with PF-475 at doses of 2.5 mg/kg, 5 mg/kg and 10 mg/kg a significant reduction of these pro-inflammatory markers was observed compared to MPTP-injected animals, in a dose-dependent manner. Furthermore, ELISA assay revealed that IL-1 β concentration increased in the colon of PD mice compared to sham animals, while PF-475 treatment was able to significantly reduce, in a dose-dependent manner, the levels of the pro-inflammatory cytokine compared with PD mice (figure 5 panel C). In contrast to the data obtained in the colon, in bowel tissues we observed that MPTP-injected mice had a slight but non-

significant increase in pro-inflammatory markers such as iNOS, COX-2 in comparison with sham mice (figure 5 panel D and E, see densitometric analysis panel D1 and E1, respectively). Furthermore, treatment with PF-475 at all administered doses did not show significant results in reducing the expression of iNOS, COX-2. Similarly, IL-1 β levels were increased but not significantly in MPTP mice compared to sham animals, while PF-475 treatment at all doses was unable to modulate the levels of this pro-inflammatory cytokine in bowel tissue (Fig. 5 panel F). In summary, these results suggested that MPTP caused severe inflammation in the colon, but less in the intestine. In addition, administration of the selective LRRK2 antagonist showed greater efficacy in reducing the levels of pro-inflammatory markers in colon tissues than in the intestine. Based on this finding, we further continued the study of LRRK2 inhibitory function in colon sections.

Figure 5: Effect of PF-475 on pro-inflammatory response induced by MPTP intoxication in colon and bowel tissues. Representative Western blot of pro-inflammatory enzyme iNOS and COX-2 in cytosolic fraction of colon tissues after MPTP and PF-475 treatments (A,B), see densitometric analysis (A1, B1, respectively). ELISA method was performed for detection of IL-1 β in cytosolic fraction of colon tissues (C). see densitometric analysis (D1, E1, respectively). ELISA method was performed for detection of IL-1 β in cytosolic fraction of bowel tissues

(F). Data are representative of at least three independent experiments. Values are means \pm SEM. One-way ANOVA test. * $p < 0.05$ vs Sham *** $p < 0.001$ vs Sham; ## $p < 0.01$ vs MPTP; ### $p < 0.001$ vs MPTP.

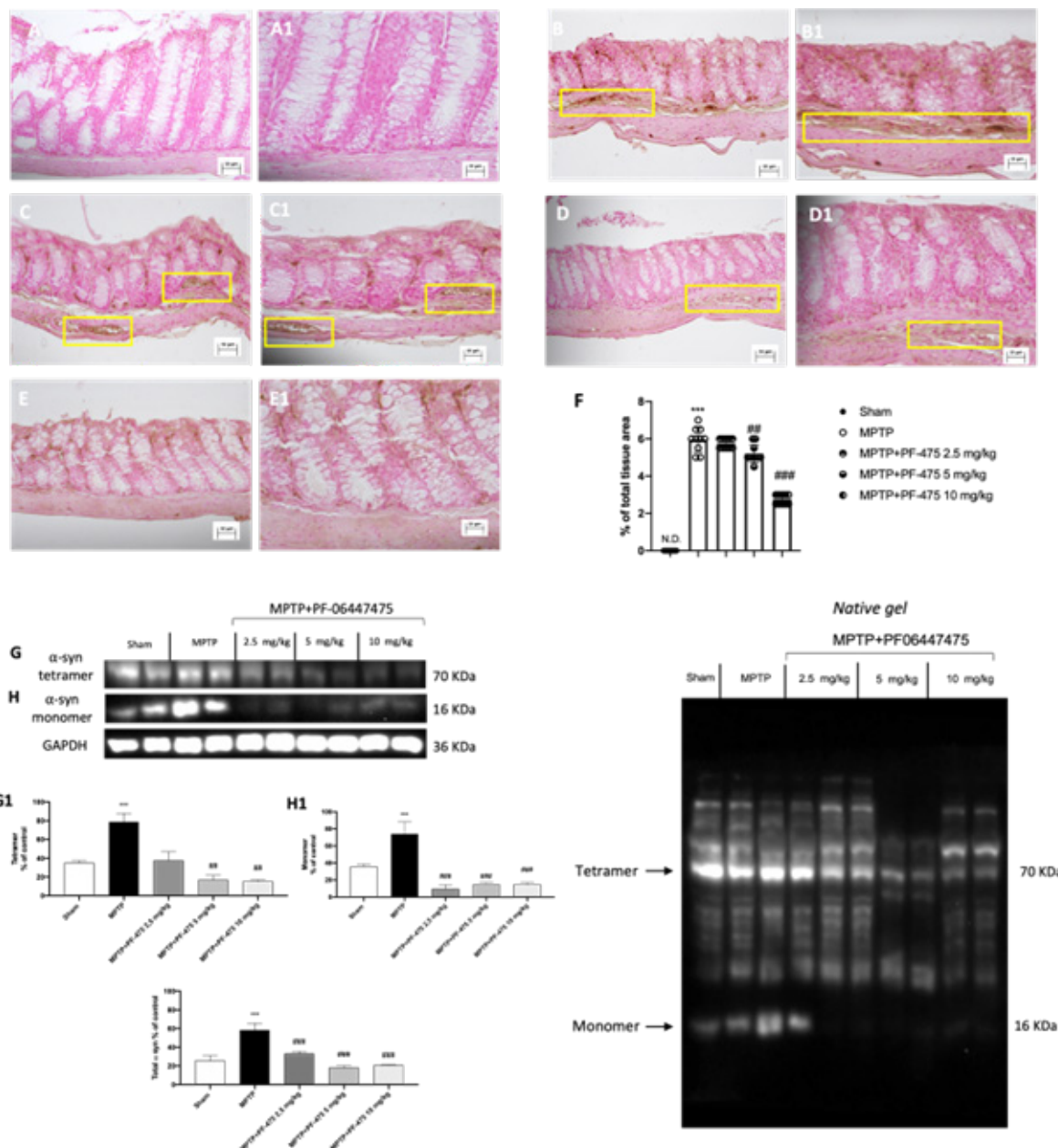


4.6. PF-475 Reduced α -Synuclein Accumulation In The Colon Of PD Mice

It has been reported that during PD, colonic dysfunction associated with dopaminergic degeneration in the enteric nervous system is closely related to an increase in α -synuclein, which is found in the colon of PD patients [26]. In our study, through immunohistochemical analysis, we estimated the number of α -synuclein-positive enteric cells in the colon of MPTP-injected mice to evaluate whether PF-475 could reduce its accumulation. In our study, through immunohistochemical analysis, we estimated the number of α -synuclein-positive enteric cells in the colon of MPTP-injected mice to evaluate whether PF-475 could reduce its accumulation. The results showed that MPTP injection (figure 6 panel B, 20x magnification B1, see score panel F) led to an accumulation of α -synuclein in the colonic submucosa compared to sham animals (figure 6 panel A, 20x magnification A1, see score panel F). However, PF-475 at the dose of 5 mg/kg (figure 6 panel C, 20x magnification C1, see score panel F) and 10 mg/kg (figure 6 panel D, 20x magnification D1, see score panel F) protected enteric dopaminergic neurons from MPTP by significantly reducing the number of α -synuclein positive cells compared to PD mice. In addition, the result was confirmed by Western blot analysis which revealed an accumulation of different forms of α -syn, including tetrameric (figure 6 panel G, see densitometric analysis panel G1) and

monomeric (figure 6 panel H, see densitometric analysis panel H1) in the colon of mice MPTP injected versus sham animals. Treatment with PF-475 significantly reduced α -synuclein tetramer at all doses compared to MPTP mice (figure 6 panel G, see densitometric analysis panel G1). Otherwise, PF-475 treatment reduced α -synuclein monomer at doses of 5 mg/kg and 10 mg/kg compared to MPTP mice. In each case the densitometric analysis of total α -synuclein (figure 6 panel I) demonstrated that PF-475 at all administered doses significantly reduced total α -synuclein levels in colonic tissues compared to MPTP animals.

Figure 6: PF-475 treatment preserved α -Syn accumulation in colon tissue. Immunohistochemical localization of α -syn after MPTP in colon tissue. Sham group (A, A1; see score F), MPTP group (B, B1; see score F), PF-475 2,5 mg/kg treatments after MPTP (C, C1; see score F), PF-475 5 mg/kg treatments after MPTP (D, D1; see score F) and PF-475 10 mg/kg treatments after MPTP (E, E1; see score F). Representative Western blot of α -syn tetramer and monomer protein expression level in colon tissues after MPTP intoxication and PF-475 treatments (G,H; see densitometric analysis G1, H1, respectively). Data are representative of at least three independent experiments. Values are means \pm SEM. One-way ANOVA test. *** $p < 0.001$ vs Sham; ## $p < 0.01$ vs MPTP; ### $p < 0.001$ vs MPTP.



4.7 LRRK2 Antagonist, PF-475, Modulated Enteric Nervous System In MPTP-Injected Mouse Colon

During PD pathogenesis, the reduction of enteric nervous system proteins present in the colon have often been associated with constipation phenomena and intestinal permeability alterations. Among these proteins, NSE and PGP9.5 represent the main markers of enteric neural cells [27]. Expression levels of PGP9.5 and NSE were significantly reduced in PD mice compared to sham mice (figure 7 panel A and B, see densitometric analysis panel A1 and B1, respectively). In contrast, intraperitoneal treatment with PF-475 at the doses of 5 mg/kg and 10 mg/kg considerably restored the expression of PGP9.5 compared to MPTP mouse (figure 7 panel A, see densitometric analysis panel A1). Whereas intraperitoneal treatment with PF-475 at the highest dose of 10 mg/kg increased enteric neuronal marker NSE compared to MPTP mouse (figure 7 panel B, see

densitometric analysis panel B1). In addition, the distribution of neural population of PGP9.5 proteins was observed in immunohistochemistry analysis to confirm whether the Western blot results were well reflected. Interestingly, PGP9.5-positive neuronal cells were strongly reduced in colonic sections of MPTP-injected mice (figure 7 panel D, 20x magnification D1, see score panel H) compared with colonic sections of sham mice (figure 7 panel C, 20x magnification C1, see score panel H). Selective inhibition of LRRK2 significantly reduced the loss of PGP 9.5 positive cells showing in colonic sections of mice treated with PF-475, at the higher dose of 10mg/kg an increase in PGP 9.5 positive cells in the submucosal layer and the muscle layer (figure 7 panel G, 20x magnification G1, see score panel H) compared to MPTP-injected mice. These results provide a basis for unveiling that selective LRRK2 inhibition in the colon also modulates enteric nervous system markers during synucleinopathies.

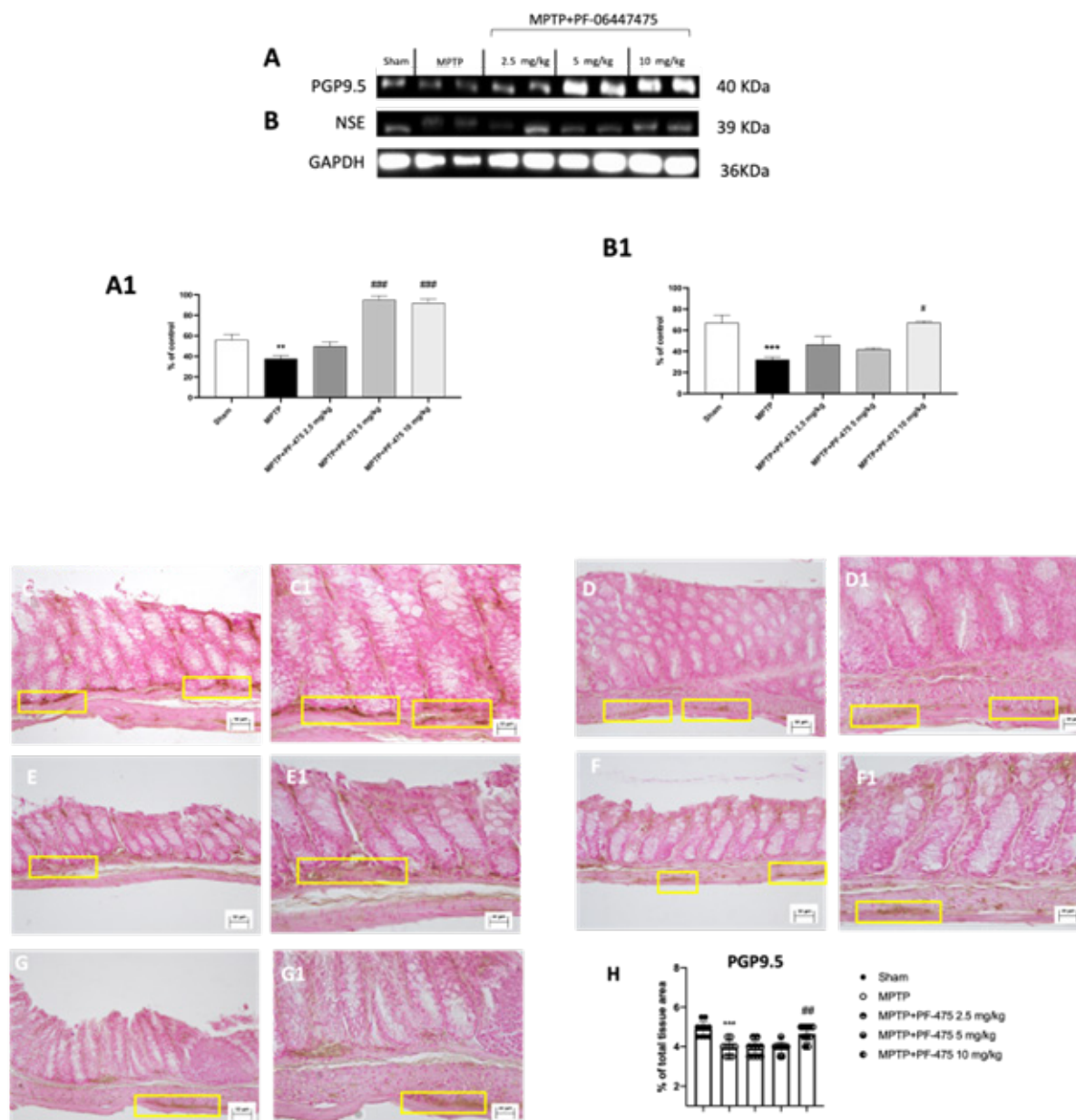


Figure 7: Effect of PF-475 on enteric nervous system in MPTP-injected mouse colon.

Representative Western blot of enteric nervous system proteins such as PGP9.5 and NSE in cytosolic fraction of colon tissues after MPTP and PF-475 treatments (A, B), see densitometric analysis (A1, B1, respectively). Immunohistochemical localization of PGP9.5 after MPTP intoxication in colon tissue. Sham group (C, C1; see score H), MPTP group (D, D1; see score H), PF-475 2.5 mg/kg treatments after MPTP (E, E1; see score H), PF-475 5 mg/kg treatments after MPTP (F, F1; see score H) and PF-475 10 mg/kg treatments after MPTP (G, G1; see score F). Data are representative of at least three independent experiments. Values are means \pm SEM. One-way ANOVA test. ** < 0.01 vs Sham; ***p < 0.001 vs Sham; # p < 0.05 vs MPTP; ### p < 0.01 vs MPTP; ####p < 0.001 vs MPTP.

4.8. PF-475 Reduced Colon Inflammation Through Mitophagy Pathway

The dysfunction of autophagic pathways characteristic of neurodegeneration in PD is also strongly implicated in inflammatory bowel disease, leading to impaired intestinal epithelial barrier function, disrupted microbiome, and defective antibacterial peptide secretion. Furthermore, substantial evidence indicates that LRRK2 mutations play a key role in the autophagy/lysosomal pathway linking PD to intestinal dysfunction [28-30]. Therefore, once we demonstrated the beneficial role of PF-475 in activating the mitophagy pathway in the brain, we aimed to investigate whether LRRK2 inhibition could modulate this pathway also in the colon of mouse with PD. Consistent with the data obtained in brain tissues, MPTP induced an alteration of autophagic processes also in the colon. Particularly, western blot analysis was performed to investigate the selective mitophagy receptors such as OPTN, p62 and

LAMP2 involved in the recognition of the ubiquitinated cargo to connect it to the autophagosome membrane. Our results demonstrated a significant reduction of OPT and LAMP2 (figure 8 panel A and B, see densitometric analysis panel A1 and B1, respectively) and an increase of p62 (figure 8 panel C, see densitometric analysis panel C1) in colon tissues of PD mice compared to sham animals. However, PF-475 treatment improved mitophagy by increasing OPT, and LAMP2 expression and reducing P62. Particularly, PF-475 at all administered doses significantly increased OPT expression levels compared to MPTP-injected mice, while only higher doses of PF-475 (5 mg/kg and 10 mg/kg) were able to significantly increase LAMP2 levels compared to MPTP mice. In contrast, PF-475 treatment, at

all doses, reduced p62 compared to MPTP mice. Furthermore, we also wanted to evaluate TNF- α which is a major pro-inflammatory cytokine, that accelerates intestinal damage. As shown in Fig. 8 panel D, the levels of this cytokine were significantly increased after administration of MPTP compared to sham mice. Consistently, the increase in production of this cytokine in colonic tissues was suppressed in a dose-dependent manner following the administration with PF-475 at a dose of 2.5 mg/kg, 5 mg/kg and 10 mg/kg compared to MPTP-injected mice (figure 8 panel D, see densitometric analysis panel D1). Taken together, our data confirmed that the resolution of MPTP-induced intestinal damage could be closely related to autophagy activation mediated by LRRK2 inhibition.

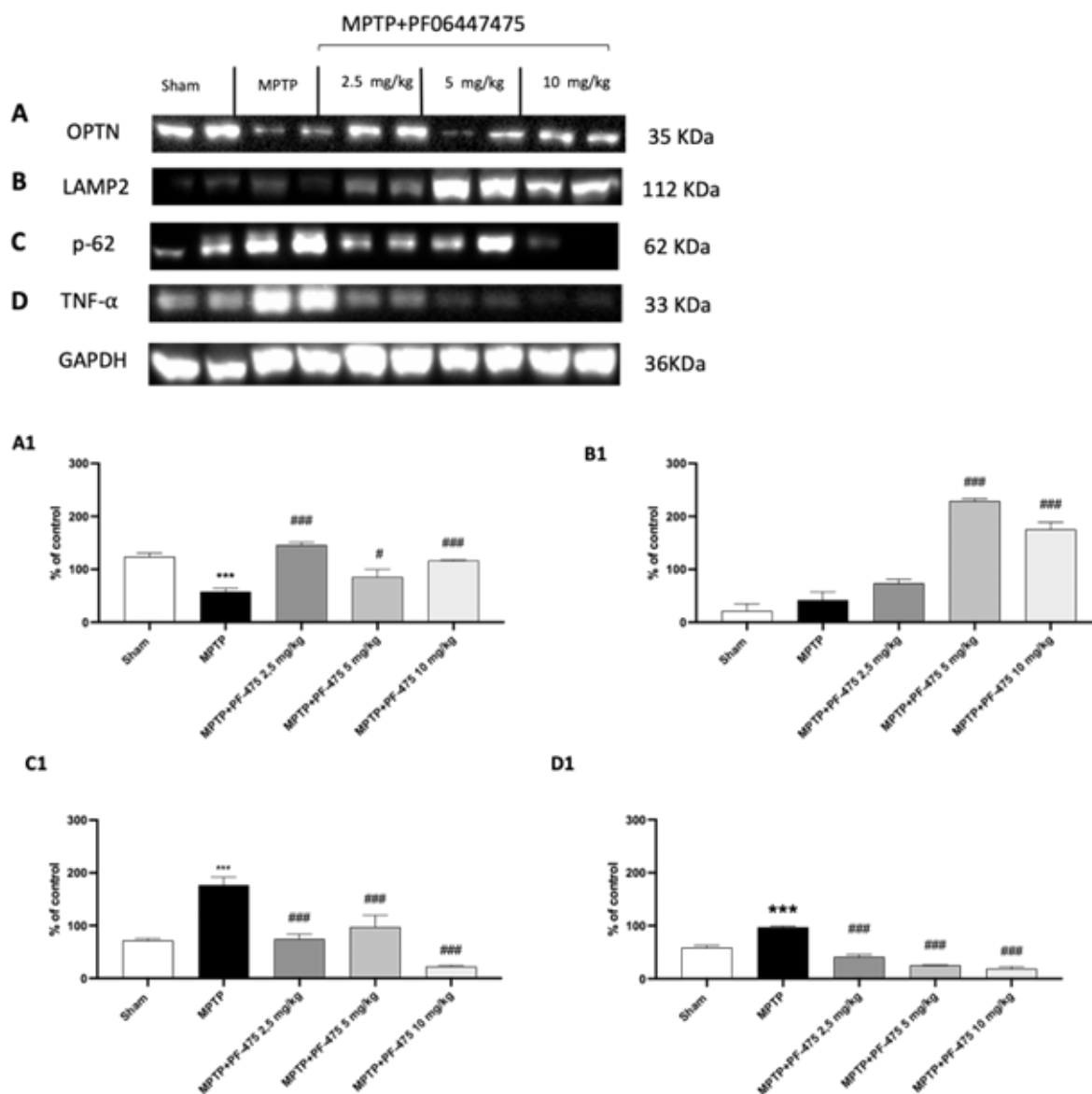


Figure 8: Effect of PF-475 on mitophagy pathway in MPTP-injected mouse colon. Cytosolic fractions of colon tissues were used to evaluate mitophagic protein expression such as OPT, LAMP2 and p62 and pro-inflammatory cytokine TNF- α after MPTP intoxication and PF-475 treatments. Representative Western blot of mitophagic protein are shown (A, B, C), see densitometric analysis (A1, B1 and C1, respectively). Expression levels of pro-inflammatory cytokine TNF- α are shown (D, see densitometric analysis D1). Data are representative of at least three independent experiments. Values are means \pm SEM. One-way ANOVA test. *** p < 0.001 vs Sham; # p < 0.05 vs MPTP; ### p < 0.001 vs MPTP.

4.9 PF-475 Reverse Alterations In Intestinal Barrier Function In Colon Of MPTP Mice

Since several studies demonstrated that PD patients had high intestinal permeability related to the disorganization of tight junction proteins [31, 32], we investigated, by immunofluorescence analysis, the effects of PF-475 on the modulation of zonula occluden-1 (ZO-1) and occludin that are pivotal proteins that regulate the paracellular permeability in intestinal epithelial cells. In this study, we demonstrated that, in colon tissue, MPTP induced a significant decrease in the number of ZO-1 (Fig. 9 panel B, see score panel F) and occludin-positive cells (Fig. 9 panel H, see score panel L) compared to sham animals (Fig. 9 panel A and G, see score panel F and L). However, PF-475 treatments at the doses of 5 mg/kg and 10 mg/kg increased the number of occludin (Fig. 9 panel D and E, see score panel F) and ZO-1 positive cells (Fig. 9 panel J and K, see score panel L) compared to MPTP-injected mice, suggesting that selective LRRK2 inhibition might protect against the intestinal barrier effects of MPTP in the colon. Intestinal permeability and integrity can be also measured by the evaluation of passive absorption of monosaccharides [33]. Therefore, in this study, we decided to detect Lactulose/Mannitol (Lac/Man) ratio to assess gut permeability. Our results demonstrated that mice subjected to MPTP intoxication showed an increased gut permeability as observed by the increased Lactulose/Mannitol (Lac/Man) ratio compared to sham mice (Figure 9 panel M). However, PD mouse treated with PF-475 showed a significant reduction of the Lac/Man ratio at the doses of 5 mg/kg and 10 mg/kg (Figure 9 panel N). To further assess gut permeability a TEER test was performed under ex vivo conditions (figure 9 panel N). Exposure of colonic cells to MPTP resulted in a decrease in TEER compared with control cells. On the other hand, TEER values significantly increased in PF-475-treated cells at the concentrations of 1 and 3 mM compared with MPTP cells. Furthermore, intraperitoneal injection of the neurotoxin MPTP caused delayed transit and constipation, as demonstrated by daily stool weight analysis (figure 9 panel O). After five days of treatment with PF-475 stool weight was not significantly affected. In contrast, after six and seven days of treatment with PF-475 at the doses of 5 mg/kg and 10 mg/kg the stool weight was significantly increased, compared with the MPTP-injected mice. Thus, PF-47 significantly reduced the alteration of gut permeability in MPTP mouse, restoring the normal intestinal integrity.

5. Discussion

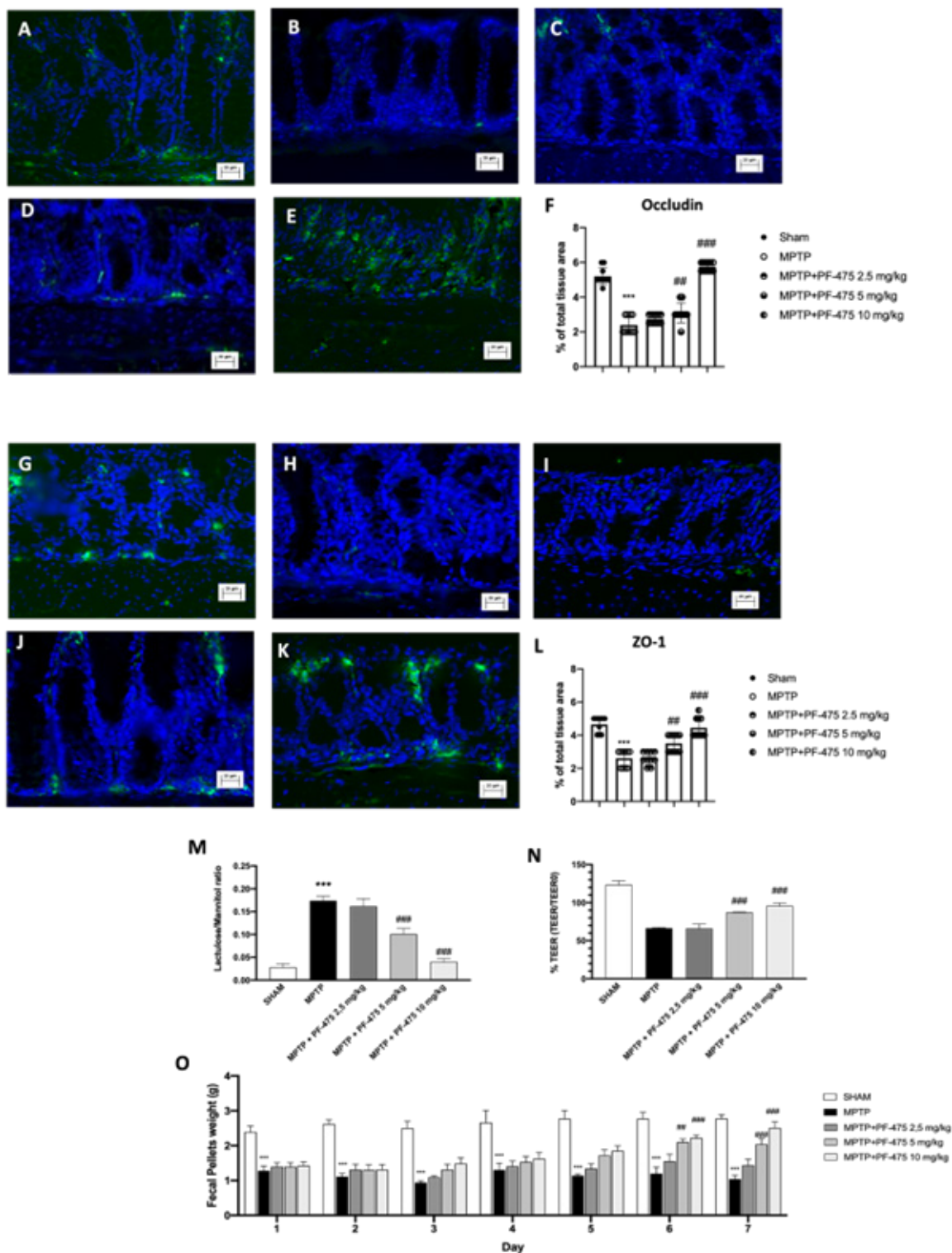
Since LRRK2 is a kinase widely and ubiquitously expressed in immune cells, blood cells, gut lumen, and neuronal cells, it has been thought to be one of the predictive risk factors for PD, inflammatory bowel disease (IBD), Crohn's disease (CD) and also tumors [4, 34,35]. We confirmed increased LRRK2 expression in the brains of PD mice, which is consistent with the elevated expression of LRRK2 [23] in the bowel and colon of PD mice. Indeed, LRRK2 contributed to the intestinal and colon impairments while LRRK2 downregulation by using PF-06447475 inhibitor displayed less serious gastrointestinal consequences after MPTP injection than control mice successfully suggesting an improvement of gastrointestinal system functionality. Although the primary mechanism

of PD pathogenesis is still unclear, mitochondrial dysfunction has been increasingly confirmed to be a dynamic contributor. That is because neurotoxins injection to reproduce PD models, including MPTP, damages mitochondrial function by inhibiting its complex core activity and causing the activation of mitophagy to degrade organelles and misfolded proteins. Our observations go further with the alterations in CNS postulating that PD originates in the gastrointestinal tract and that the appearance of a-synuclein accumulation initially occurs, in the earliest stage of PD, in the enteric nervous system (ENS). Indeed, LRRK2 inhibition in bowel and colon of PD mice protected gastrointestinal system from intestinal inflammation mediated by NF- κ B that was interestingly enhanced by MPTP and that was inversely decreased from LRRK2 inhibition, indicating that LRRK2 down regulation is controlled in NF- κ B -dependent manner. Moreover, through mitophagy, altered intestinal cells regulate both the number and quality of mitochondria in response to the toxic stress from MPTP injection [36]. Our study shows that the damaged colonocytes in the colonic tissue are susceptible from MPTP and that results in a modulation of mitophagy driven by OPTN, LAMP-2 and p62 present in enteric neuronal mitochondria and TNF- α interacts with mitophagy by mediating its functionality. As such, OPTN is frequently increased not only in the protein inclusions of PD neurons mainly because defective mitophagy, leading to neurodegeneration but also in gastrointestinal system implicating a role in intestinal homeostasis and disease [37]. Therefore, inhibition of LRRK2 has a direct role in inflammation and in mitoautophagic functions by positively regulate mitochondrial dynamics and autophagosome-lysosome fusion. Here, this was accompanied by an increase in autophagic flux and higher expression of mitophagy markers in mice treated with LRRK2 inhibitor. To date, little is known about the role of PGP9.5 in PD. However, high levels of UCH-L1 expression were found in LBs throughout the central and peripheral nervous systems at all stages of PD.

Figure 9: Effect of PF-475 on intestinal barrier function in colon tissue.

Immunofluorescence analysis of occludin and ZO-1. Colon sections were stained with antibodies against occludin (green) or ZO-1 (green) and DAPI to highlight cell nuclei (blue). Occludin + cells in sham group (A, A1); see mean of intensity fluorescence (F). No Occludin + cells were showed in mice subjected to MPTP (B, B1); see mean of intensity fluorescence (F). Mice treated with PF-475 at doses of 2,5 mg/kg (C, C1) see mean of intensity fluorescence (F), and 5 mg/kg (D, D1); see mean of intensity fluorescence (F) and 10 mg/kg (E, E1); see mean of intensity fluorescence (F). ZO-1 + cells in sham group (G, G1); see mean of intensity fluorescence (L). No ZO-1+ cells were showed in mice subjected to MPTP (H, H1); see mean of intensity fluorescence (L). Mice treated with PF-475 at doses of 2,5 mg/kg (I, I1) see mean of intensity fluorescence (L), and 5 mg/kg (J, J1); see mean of intensity fluorescence (L) and 10 mg/kg (K, K1); see mean of intensity fluorescence (L). The barrier-protective effect of PF-475 on colonic cells were assessed through Lac/Man test (M) and the TEER test (N). Constipation-related indicator was assessed through determination of fecal weight (O). Data are representative of at least three

independent experiments. Values are means \pm SEM. One-way ANOVA test. *** $p < 0.001$ vs Sham; ## $p < 0.01$ vs MPTP; ### $p < 0.001$ vs MPTP.



PGP9.5 belongs to the ubiquitin COOH-terminal hydrolase family and its alteration triggers the stability of the ubiquitin-dependent proteolytic system [27, 38]. In our data, we found that the expression of PGP9.5 was reduced by MPTP exposure and this is accompanied by changes in the density of NSE in colonic tissue. In colonic tissue, LRRK2 inhibition leads to a significant decrease in PGP9.5 and NSE expression along with

the restoration of PD-related colon dysfunctions by showing them as a strong predictor of PD outcome. Consistently with studies about LRRK2 inhibitors and LRRK2^{-/-} mice [4, 39] effectively we found ameliorations in colon dysfunction of PD mice by using PF-475, and that is because of its exerting action to modulate mitophagy also in colon tissue. We found an abnormal mitochondrial dynamic in the colon of PD-mice, a

process that basically influences mitochondrial function and autophagy all implicated also in IBD [40]. In the present study, MPTP induction significantly activated mitophagy markers including LAMP2, OPTN, p62 and TNF- expression levels in colon tissues. Also, markers to monitor mitophagy were decreased by LRRK2 inhibition by acting as an upstream coordinator of the degradative process. As changes in mitophagy have been found in the colon of PD mice and after LRRK2 inhibition, dysfunctions of colon epithelial cells are often accompanied by impairments of barrier integrity and function. In this perspective, the evaluation of tight junctions represented by Occludin, and ZO-1 allowed us to confirm that PD triggers in alterations of colon integrity and to discover the contribution of LRRK2 in rebalancing colon barrier alteration from consequent damage. Maintenance of TJ integrity is energy-dependent, and that is not a surprise being mitochondria damaged [41]. Indeed, the disruption of colon permeability has been found in the colon of PD-mice with a reduction of colonic absorption because colonic bacteria metabolize lactulose and mannitol molecules. In the opposite direction, the decrease of colonic permeability is rebalanced by LRRK2 inhibitor PF-475 showing that lactulose/mannitol ratio passed through the colonic tissue and this is indicative of the relevance of the inhibitor action in modulating colonic permeability. Moreover, PD triggers colonic barrier integrity alterations that were detectable by trans-epithelial electrical resistance (TEER) measurements [42]. In our hands, the state of barrier integrity of the PD-mice colon tissue was affected by MPTP injection and the paracellular passage of molecules was altered, while PF-475 effects were completely able to restore barrier integrity following its administration demonstrating that blocking LRRK2 with the specific antagonist was sufficient to restore the impaired barrier function in colonic tissue of PD-mice.

6. Conclusions

Given the multiple cellular mechanisms of LRRK2 that are dysfunctional in SNpc, and in the colon of PD mice, enhancing mitophagy and improving tissue restoration may rescue PD progression and related diseases. Here, we provided different several lines of evidence that treatment with LRRK2 inhibitor wick improve colon barrier and integrity attenuate PD-related symptoms and progression.

References

- Shults CW. Lewy bodies. *Proc Natl Acad Sci U S A*. 2006; 103(6): 1661-8.
- Fasano A, Visanji NP, Liu LW, Lang AE, Pfeiffer RF. Gastrointestinal dysfunction in Parkinson's disease. *Lancet Neurol*. 2015; 14(6): 625-39.
- Bu J, Liu J, Liu K, Wang Z. Diagnostic utility of gut alpha-synuclein in Parkinson's disease: A systematic review and meta-analysis. *Behav Brain Res*. 2019; 364: 340-7.
- Yan J, Yu W, Wang G, Lu C, Liu C, Jiang L, et al. LRRK2 deficiency mitigates colitis progression by favoring resolution of inflammation and restoring homeostasis of gut microbiota. *Genomics*. 2022; 114(6): 110527.
- Price A, Manzoni C, Cookson MR, Lewis PA. The LRRK2 signalling system. *Cell Tissue Res*. 2018; 373(1): 39-50.
- Giltsbach BK, Messias AC, Ito G, Sattler M, Alessi DR, Wittinghofer A, et al. Structural Characterization of LRRK2 Inhibitors. *J Med Chem*. 2015; 58(9): 3751-6.
- Chu CT. A pivotal role for PINK1 and autophagy in mitochondrial quality control: implications for Parkinson disease. *Hum Mol Genet*. 2010; 19(R1): R28-37.
- Johansen T, Lamark T. Selective autophagy mediated by autophagic adapter proteins. *Autophagy*. 2011; 7(3): 279-96.
- Filippone A, Mannino D, Cucinotta L, Paterniti I, Esposito E, Campolo M. LRRK2 Inhibition by PF06447475 Antagonist Modulates Early Neuronal Damage after Spinal Cord Trauma. *Antioxidants (Basel)*. 2022;11(9).
- Liberatore GT, Jackson-Lewis V, Vukosavic S, Mandir AS, Vila M, McAuliffe WG, et al. Inducible nitric oxide synthase stimulates dopaminergic neurodegeneration in the MPTP model of Parkinson disease. *Nat Med*. 1999; 5(12): 1403-9.
- Ardizzone A, Filippone A, Mannino D, Scuderi SA, Casili G, Lanza M, et al. Ulva pertusa, a Marine Green Alga, Attenuates DNBS-Induced Colitis Damage via NF-kappaB/Nrf2/SIRT1 Signaling Pathways. *J Clin Med*. 2022; 11(15): 4301.
- Ardizzone A, Mannino D, Capra AP, Repici A, Filippone A, Esposito E, et al. New Insights into the Mechanism of Ulva pertusa on Colitis in Mice: Modulation of the Pain and Immune System. *Mar Drugs*. 2023; 21(5): 298.
- Scuderi SA, Casili G, Lanza M, Ardizzone A, Pantaleo L, Campolo M, et al. Efficacy of a Product Containing Xyloglucan and Pea Protein on Intestinal Barrier Function in a Partial Restraint Stress Animal Model. *Int J Mol Sci*. 2022; 23(4): 2269.
- Lee HY, Kim JH, Jeung HW, Lee CU, Kim DS, Li B, et al. Effects of Ficus carica paste on loperamide-induced constipation in rats. *Food Chem Toxicol*. 2012; 50(3-4): 895-902.
- Haddad MJ, Sztupecki W, Delayre-Orthez C, Rhazi L, Barbezier N, Depeint F, et al. Complexification of In Vitro Models of Intestinal Barriers, A True Challenge for a More Accurate Alternative Approach. *Int J Mol Sci*. 2023; 24(4): 3595.
- Singh F, Ganley IG. Parkinson's disease and mitophagy: an emerging role for LRRK2. *Biochem Soc Trans*. 2021; 49(2): 551-62.
- Wauters F, Cornelissen T, Imberechts D, Martin S, Koentjoro B, Sue C, et al. LRRK2 mutations impair depolarization-induced mitophagy through inhibition of mitochondrial accumulation of RAB10. *Autophagy*. 2020; 16(2): 203-22.
- Wu F, Xu HD, Guan JJ, Hou YS, Gu JH, Zhen XC, et al. Rotenone impairs autophagic flux and lysosomal functions in Parkinson's disease. *Neuroscience*. 2015; 284: 900-11.
- Jin MM, Wang F, Qi D, Liu WW, Gu C, Mao CJ, et al. A Critical Role of Autophagy in Regulating Microglia Polarization in Neurodegeneration. *Front Aging Neurosci*. 2018; 10: 378.
- Hui KY, Fernandez-Hernandez H, Hu J, Schaffner A, Pankratz N,

- Hsu NY, et al. Functional variants in the LRRK2 gene confer shared effects on risk for Crohn's disease and Parkinson's disease. *Sci Transl Med.* 2018; 10(423).
21. Herrick MK, Tansey MG. Is LRRK2 the missing link between inflammatory bowel disease and Parkinson's disease? *NPJ Parkinsons Dis.* 2021; 7(1): 26.
 22. Cote M, Bourque M, Poirier AA, Aube B, Morissette M, Di Paolo T, et al. GPER1-mediated immunomodulation and neuroprotection in the myenteric plexus of a mouse model of Parkinson's disease. *Neurobiol Dis.* 2015; 82: 99-113.
 23. Devos D, Lebouvier T, Lardeux B, Biraud M, Rouaud T, Pouclet H, et al. Colonic inflammation in Parkinson's disease. *Neurobiol Dis.* 2013; 50: 42-8.
 24. Cote M, Poirier AA, Aube B, Jobin C, Lacroix S, Soulet D. Partial depletion of the proinflammatory monocyte population is neuroprotective in the myenteric plexus but not in the basal ganglia in a MPTP mouse model of Parkinson's disease. *Brain Behav Immun.* 2015; 46: 154-67.
 25. Cote M, Drouin-Ouellet J, Cicchetti F, Soulet D. The critical role of the MyD88-dependent pathway in non-CNS MPTP-mediated toxicity. *Brain Behav Immun.* 2011; 25(6): 1143-52.
 26. Natale G, Kastsiuchenka O, Pasquali L, Ruggieri S, Paparelli A, Fornai F. MPTP- but not methamphetamine-induced parkinsonism extends to catecholamine neurons in the gut. *Ann N Y Acad Sci.* 2008; 1139: 345-9.
 27. Choi YJ, Song HJ, Kim JE, Lee SJ, Jin YJ, Roh YJ, et al. Dysregulation of the Enteric Nervous System in the Mid Colon of Complement Component 3 Knockout Mice with Constipation Phenotypes. *Int J Mol Sci.* 2022; 23(12).
 28. Zhang K, Zhu S, Li J, Jiang T, Feng L, Pei J, et al. Targeting autophagy using small-molecule compounds to improve potential therapy of Parkinson's disease. *Acta Pharm Sin B.* 2021; 11(10): 3015-34.
 29. Smolders S, Van Broeckhoven C. Genetic perspective on the synergistic connection between vesicular transport, lysosomal and mitochondrial pathways associated with Parkinson's disease pathogenesis. *Acta Neuropathol Commun.* 2020; 8(1): 63.
 30. Sosero YL, Gan-Or Z. LRRK2 and Parkinson's disease: from genetics to targeted therapy. *Ann Clin Transl Neurol.* 2023; 10(6): 850-64.
 31. Forsyth CB, Shannon KM, Kordower JH, Voigt RM, Shaikh M, Jaglin JA, et al. Increased intestinal permeability correlates with sigmoid mucosa alpha-synuclein staining and endotoxin exposure markers in early Parkinson's disease. *PLoS One.* 2011; 6(12): e28032.
 32. Clairembault T, Leclair-Visonneau L, Coron E, Bourreille A, Le Dily S, Vavasseur F, et al. Structural alterations of the intestinal epithelial barrier in Parkinson's disease. *Acta Neuropathol Commun.* 2015; 3: 12.
 33. Volynets V, Reichold A, Bardos G, Rings A, Bleich A, Bischoff SC. Assessment of the Intestinal Barrier with Five Different Permeability Tests in Healthy C57BL/6J and BALB/cJ Mice. *Dig Dis Sci.* 2016; 61(3): 737-46.
 34. Dickson DW, Braak H, Duda JE, Duyckaerts C, Gasser T, Halliday GM, et al. Neuropathological assessment of Parkinson's disease: refining the diagnostic criteria. *Lancet Neurol.* 2009; 8(12): 1150-7.
 35. Jiang ZC, Chen XJ, Zhou Q, Gong XH, Chen X, Wu WJ. Downregulated LRRK2 gene expression inhibits proliferation and migration while promoting the apoptosis of thyroid cancer cells by inhibiting activation of the JNK signaling pathway. *Int J Oncol.* 2019; 55(1): 21-34.
 36. Wang B, Abraham N, Gao G, Yang Q. Dysregulation of autophagy and mitochondrial function in Parkinson's disease. *Transl Neurodegener.* 2016; 5: 19.
 37. Wise JP, Price CG, Amaro JA, Cannon JR. Autophagy Disruptions Associated With Altered Optineurin Expression in Extranigral Regions in a Rotenone Model of Parkinson's Disease. *Front Neurosci.* 2018; 12: 289.
 38. Satoh JI, Kuroda Y. Ubiquitin C-terminal hydrolase-L1 (PGP9.5) expression in human neural cell lines following induction of neuronal differentiation and exposure to cytokines, neurotrophic factors or heat stress. *Neuropathol Appl Neurobiol.* 2001; 27(2): 95-104.
 39. Takagawa T, Kitani A, Fuss I, Levine B, Brant SR, Peter I, et al. An increase in LRRK2 suppresses autophagy and enhances Dectin-1-induced immunity in a mouse model of colitis. *Sci Transl Med.* 2018; 10(444).
 40. Liang D, Zhuo Y, Guo Z, He L, Wang X, He Y, et al. SIRT1/PGC-1 pathway activation triggers autophagy/mitophagy and attenuates oxidative damage in intestinal epithelial cells. *Biochimie.* 2020; 170: 10-20.
 41. Dickman KG, Hempson SJ, Anderson J, Lippe S, Zhao L, Burakoff R, et al. Rotavirus alters paracellular permeability and energy metabolism in Caco-2 cells. *Am J Physiol Gastrointest Liver Physiol.* 2000; 279(4): G757-66.
 42. Marrella A, Buratti P, Markus J, Firpo G, Pesenti M, Landry T, et al. In vitro demonstration of intestinal absorption mechanisms of different sugars using 3D organotypic tissues in a fluidic device. *ALTEX.* 2020; 37(2): 255-64.